

## Spatial redistribution of the optical field intensity in inverted polymer solar cells

Fang-Chung Chen, Jyh-Lih Wu, and Yi Hung

Citation: *Applied Physics Letters* **96**, 193304 (2010); doi: 10.1063/1.3430060

View online: <http://dx.doi.org/10.1063/1.3430060>

View Table of Contents: <http://scitation.aip.org/content/aip/journal/apl/96/19?ver=pdfcov>

Published by the *AIP Publishing*

---

### Articles you may be interested in

Performance improvement of inverted polymer solar cells by doping Au nanoparticles into TiO<sub>2</sub> cathode buffer layer

Appl. Phys. Lett. **103**, 233303 (2013); 10.1063/1.4840319

Increased efficiency of low band gap polymer solar cells at elevated temperature and its origins

Appl. Phys. Lett. **99**, 133302 (2011); 10.1063/1.3643450

Improved power conversion efficiency of InP solar cells using organic window layers

Appl. Phys. Lett. **98**, 053504 (2011); 10.1063/1.3549692

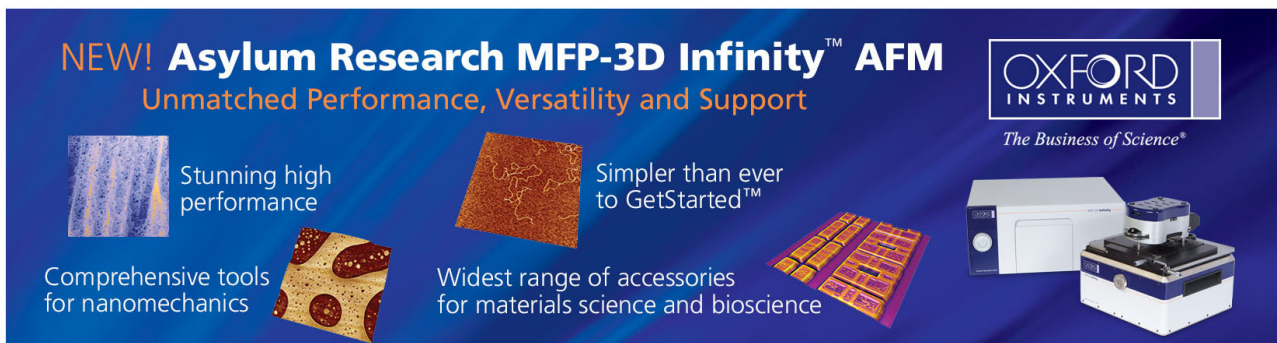
Organic solar cells with a multicharge separation structure consisting of a thin rubrene fluorescent dye for open circuit voltage enhancement

Appl. Phys. Lett. **98**, 023301 (2011); 10.1063/1.3535603

Efficient multilayer organic solar cells using the optical interference peak

Appl. Phys. Lett. **93**, 043307 (2008); 10.1063/1.2962986

---



**NEW! Asylum Research MFP-3D Infinity™ AFM**  
Unmatched Performance, Versatility and Support

**OXFORD INSTRUMENTS**  
*The Business of Science®*

Stunning high performance

Simpler than ever to GetStarted™

Comprehensive tools for nanomechanics

Widest range of accessories for materials science and bioscience

## Spatial redistribution of the optical field intensity in inverted polymer solar cells

Fang-Chung Chen,<sup>1,2,a)</sup> Jyh-Lih Wu,<sup>1,3</sup> and Yi Hung<sup>1,2</sup>

<sup>1</sup>Department of Photonics, National Chiao Tung University, Hsinchu 30010, Taiwan

<sup>2</sup>Display Institute, National Chiao Tung University, Hsinchu 30010, Taiwan

<sup>3</sup>Institute of Electro-Optical Engineering, National Chiao Tung University, Hsinchu 30010, Taiwan

(Received 7 January 2010; accepted 25 April 2010; published online 14 May 2010)

We have used indium tin oxide (ITO), a transparent conducting oxide, as an optical spacer to improve the performance of inverted polymer solar cells. The optical interference effect resulted in spatial redistribution of the optical field in the devices. Although the degree of light absorption in inverted cells was not increased, the resulting favorable distribution of photogenerated excitons probably decreased the level of exciton quenching near the electrodes. As a result, the introduction of the ITO optical spacer at an appropriate thickness increased the short-circuit current density and the overall power conversion efficiency. © 2010 American Institute of Physics. [doi:10.1063/1.3430060]

Organic photovoltaic devices (OPVs) are attracting increasing attention because of their light weight, low cost, fabrication at low temperature, semitransparency, and mechanical flexibility. Recently, polymer/fullerene bulk-heterojunction solar cells have dominated the burgeoning field of OPVs; the power conversion efficiencies (PCEs) of these devices have reached as high as 6%.<sup>1–4</sup> In particular, some OPVs featuring an inverted device architecture—eliminating the acidic poly(3,4-ethylenedioxythiophene):poly(styrene sulfonate) anodic buffer layer and the air sensitive metals—have exhibited prolonged device lifetimes.<sup>5–8</sup> Accordingly, much effort is being exerted in the quest for high-performance inverted OPVs.<sup>6–10</sup> One feasible approach toward highly efficient devices is the exploitation of light trapping techniques.<sup>11–13</sup> Among them, the incorporation of an optical spacer, which redistributes the optical field spatially in the active layer, can improve the PCEs of OPVs having regular device architectures.<sup>4,14–16</sup> Nevertheless, relevant studies of the optical interference effect in inverted OPVs remain rare so far.<sup>17</sup>

In this study, we explored the effect of incorporating indium tin oxide (ITO) as an optical spacer on the performance of inverted OPV devices. The prerequisites for a functional optical spacer in OPVs include high electrical conductivity (to avoid the increased device resistance), high optical transparency, and alignment of the energy levels of the involved layers. ITO appears to be a suitable candidate for use as an optical spacer between the organic active layer and the top electrode in the inverted OPVs—except that its work function (approximately 4.7 eV) (Ref. 18) somehow misaligns with the highest occupied molecular orbital of poly(3-hexylthiophene) (approximately 5.2 eV).<sup>18</sup> This problem could be easily solved, however, by incorporating high-work-function molybdenum trioxide (MoO<sub>3</sub>; approximately 5.3 eV) (Ref. 18) as an interlayer to match the energy levels.<sup>10,18</sup> Our results of this MoO<sub>3</sub>/ITO “bilayer structure” revealed that the introduction of the ITO optical spacer notably enhanced the photocurrent, thereby increasing the over-

all device efficiency. More interestingly, as will be shown in this study, the optical interference effect, induced by the presence of the ITO optical spacer, remained beneficial to the device performance of inverted OPVs when optimizing the thickness of the active layer.

To fabricate the inverted OPV device, an interfacial layer of cesium carbonate (Cs<sub>2</sub>CO<sub>3</sub>; 99.995% purity from Aldrich) was spin-coated onto the ITO-coated glass substrate from a solution in 2-ethoxyethanol (2 mg/ml), followed by thermal annealing at 150 °C for 15 min.<sup>7</sup> The photoactive layer was spin-coated on top of the Cs<sub>2</sub>CO<sub>3</sub> from a blend of poly(3-hexylthiophene) (P3HT; Rieke Metals) and [6,6]-phenyl-C<sub>61</sub>-butyric acid methyl ester (PCBM; American Dye Source) dissolved in 1,2-dichlorobenzene (17 mg/ml; 17 mg/ml). After solvent annealing,<sup>19</sup> the dried film was thermally annealed at 110 °C for 15 min; the resulting film was approximately 180 nm thick. We note that the thickness of the active layer has been optimized experimentally. To complete the device, 20 nm thick MoO<sub>3</sub> and 150 nm thick Ag layers were sequentially deposited through thermal evaporation to function as the hole-collection contact. Here, Ag was used as the anodic electrode because of its high reflectance and conductivity. ITO layers of various thicknesses were inserted between the MoO<sub>3</sub> and Ag layers through rf sputtering to function as optical spacers. The device area, defined through a shadow mask, was 0.12 cm<sup>2</sup>. All of the completed devices were thermally postannealed at 140 °C for 5 min in a glovebox. The inset of Fig. 1(a) provides a schematic representation of the device architecture. The current density-voltage (*J*-*V*) characteristics of the devices were measured using a Keithley 2400 source-measure unit. The photocurrent was obtained under air mass 1.5 global (AM 1.5G) illumination from a 150 W Thermal Oriol solar simulator. The illumination intensity was calibrated using a standard Si photodiode equipped with a KG-5 filter (Hamamatsu, Inc.).<sup>20</sup> Optical modeling was performed using the optical transfer matrix formalism (TMF) approach.<sup>21</sup> The optical constants, including the refractive index (*n*) and extinction coefficient (*k*), of each layer in the device structure were obtained using the ellipsometry method. The film thickness of each layer was determined using atomic force mi-

<sup>a)</sup> Author to whom correspondence should be addressed. Electronic mail: fcchen@mail.nctu.edu.tw.

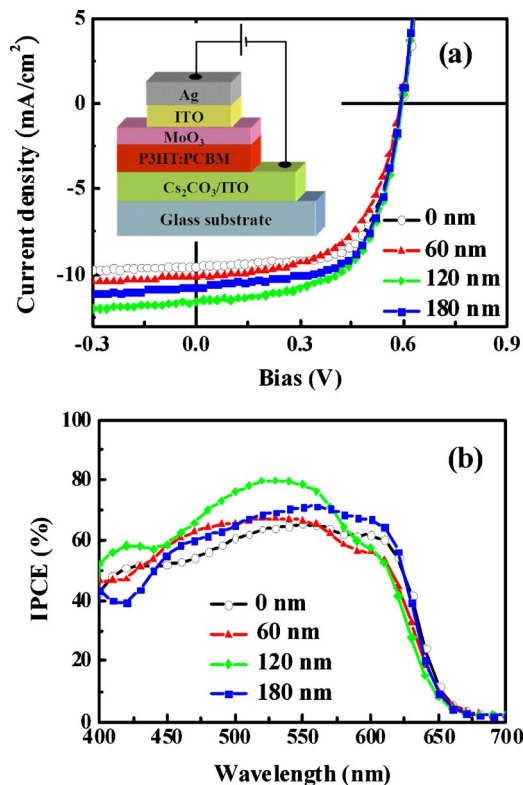


FIG. 1. (Color online) (a)  $J$ - $V$  characteristics, recorded under  $100 \text{ mW cm}^{-2}$  illumination (AM 1.5G), of polymer solar cells incorporating ITO optical spacers of various thicknesses. Inset: device architecture of OPVs incorporating an ITO optical spacer. (b) IPCE curves of polymer solar cells incorporating ITO optical spacers of various thicknesses.

crosscopy (AFM) and also confirmed employing the ellipsometry measurement.

Figure 1(a) displays the  $J$ - $V$  characteristics, recorded under  $100 \text{ mW cm}^{-2}$  illumination (AM 1.5G), of OPV devices incorporating ITO optical spacers of various thicknesses (Table I). The reference device possessing the structure ITO/Cs<sub>2</sub>CO<sub>3</sub>/P3HT:PCBM/MoO<sub>3</sub>/Ag exhibited an open-circuit voltage ( $V_{oc}$ ) of 0.59 V, a short-circuit current ( $J_{sc}$ ) of  $9.54 \text{ mA cm}^{-2}$ , and a fill factor (FF) of 0.67, yielding an overall device PCE of 3.76%. The typical photovoltaic characteristics suggested that functional (Ohmic) contacts were formed at both contacts (ITO/Cs<sub>2</sub>CO<sub>3</sub> and MoO<sub>3</sub>/Ag). Note that Cs<sub>2</sub>CO<sub>3</sub> (Refs. 5 and 7) and MoO<sub>3</sub> (Refs. 10 and 18) have been proposed to act as functional electron-selective and hole-selective layers, respectively, for efficient charge collection in OPVs. To further benefit from the optical interference effect, we inserted ITO layers of various thicknesses (60, 120, and 180 nm) between the MoO<sub>3</sub> and Ag layers. In each case, the value of  $V_{oc}$  remained at 0.59 V. In contrast, the value of  $J_{sc}$  was strongly dependent on the ITO thickness:

its optimum value occurred for an ITO thickness of 120 nm. Moreover, the FF decreased slightly after inserting the ITO optical spacers, presumably because of increased device series resistance arising from the presence of ITO<sup>22</sup> and/or possible sputtering damage. Such disadvantageous effects could, however, be overwhelmed through the incorporation of an optical spacer of a suitable thickness. The device incorporating the 120 nm thick ITO optical spacer achieved an excellent PCE of 4.20% ( $V_{oc}$ =0.59 V;  $J_{sc}$  =  $11.49 \text{ mA cm}^{-2}$ ; FF=0.62). In general, the expected performance enhancement from the optical interference effect is negated when the active layer is sufficiently thick.<sup>14,17,23</sup> Surprisingly, the inverted OPVs fabricated in this study could still benefit from the introduction of an ITO optical spacer while the thickness of the active layer was optimized.

We also compared the spectral response for devices with and without optical spacers. The incident photon-to-electron conversion efficiency (IPCE) is measured to determine the spectral response of OPVs. Figure 1(b) displays the IPCE curves for these devices. One can see that both the shape and the maximum position of spectral response changed significantly after inserting an ITO optical spacer, presumably because of the optical interference effect caused by the ITO optical spacer.

To understand the mechanism responsible for the increased values of  $J_{sc}$ , we also numerically investigated the optical interference effect of incorporating an optical spacer in OPVs through TMF optical modeling, which has been used widely to investigate the optical behavior of OPV devices.<sup>14,17,24</sup> The optical field intensity ( $|E(z)|^2$ ) at any given position in the device can be calculated from the optical constants ( $n$  and  $k$ ) and the depth of each layer. Figure 2 displays the effect of the optical spacers on the calculated distribution profiles of optical field intensity in the device at given wavelengths ( $\lambda$ ) of 500 and 550 nm. The spatial distribution of the optical field intensity was strongly dependent on the thickness of the optical spacer.

For quantitative analysis, therefore, we further calculated the distribution profiles for the exciton generation rate  $G(z)$  inside the active layer via the energy dissipation rate (Fig. 3).<sup>13,24</sup> Figure 3 reveals that the incorporation of an ITO spacer effectively tailored the distribution of photogenerated excitons. After incorporating a 120 nm thick ITO optical spacer, the values of  $G(z)$  increased within the depth range from 60 to 120 nm but decreased near both organic/electrode contacts. We suspect that the dramatic change in the distribution profile of  $G(z)$  contributed to the enhanced photocurrent.

Previously, Moulé and Meerholz<sup>25</sup> suggested that the photocurrent decreased when the light intensity in the proximity of the organic/electrode interface increased due to the

TABLE I. Photovoltaic characteristics for polymer photovoltaic devices incorporating ITO optical spacers.

ITO thickness <sup>a</sup> (nm)	$V_{oc}$ (V)	$J_{sc}$ (mA cm <sup>-2</sup> )	FF	PCE (%)
0	0.59 ( $\pm 0.01$ )	9.54 ( $\pm 0.21$ )	0.67 ( $\pm 0.02$ )	3.76 ( $\pm 0.08$ )
60	0.59 ( $\pm 0.01$ )	10.12 ( $\pm 0.31$ )	0.59 ( $\pm 0.03$ )	3.52 ( $\pm 0.21$ )
120	0.59 ( $\pm 0.01$ )	11.49 ( $\pm 0.26$ )	0.62 ( $\pm 0.02$ )	4.20 ( $\pm 0.12$ )
180	0.59 ( $\pm 0.01$ )	10.71 ( $\pm 0.25$ )	0.64 ( $\pm 0.02$ )	4.04 ( $\pm 0.11$ )

<sup>a</sup>ITO incorporated as an optical spacer.

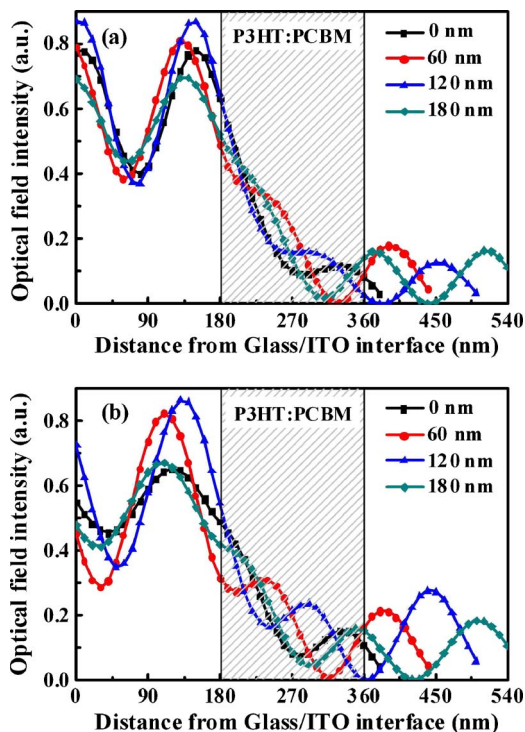


FIG. 2. (Color online) Calculated distribution profiles for the optical field intensities in OPV devices incorporating ITO optical spacers of various thicknesses, determined at wavelengths of (a) 500 and (b) 550 nm.

exciton quenching (recombination) in conventional devices. In the present study, the shift in the exciton generation zone away from the electrodes probably diminished possible exciton quenching at the electrodes. Therefore, the use of an ITO optical spacer of an appropriate thickness can give rise to a favorable distribution profile of  $G(z)$  for maximizing the number of “effective” photon-generated excitons. Finally, we note that the “optical spacers” failed to increase the amount of excitons (which can be calculated by integrating the area beneath the curves in Fig. 3) because our devices had sufficiently thick films for photon harvesting.<sup>14,17</sup> However, the favorable distribution profile of  $G(z)$  was still beneficial for

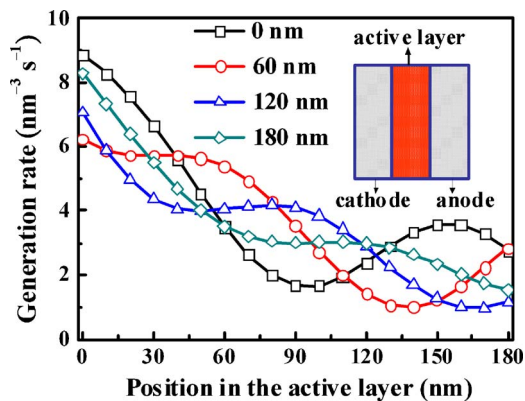


FIG. 3. (Color online) Calculated distribution profiles of the exciton generation rate inside the active layer for OPV devices incorporating ITO optical spacers of various thicknesses. Inset: schematic illustration of our layer stack.

improving the overall device efficiency of OPVs.

In conclusion, we have improved the PCE of the inverted OPVs by incorporating an ITO optical spacer, thereby achieving interference-enhanced devices. The resulting optical interference effect led to spatial redistribution of the optical field intensity and the distribution profile of exciton generation rate. Although the degree of light absorption in inverted OPVs was not increased, the resulting favorable distribution of photogenerated excitons probably decreased the level of exciton quenching near the electrodes. Our results indicate that the inverted OPVs could still benefit from such optical effects when they had a sufficiently thick active layer.

We thank the National Science Council (Grant Nos. NSC 98-3114-E-009-005 and 98-2221-E-009-028) and the Ministry of Education ATU program for financial support.

- <sup>1</sup>S. H. Park, A. Roy, S. Beaupre, S. Cho, N. Coates, J. S. Moon, D. Moses, M. Leclerc, K. Lee, and A. J. Heeger, *Nat. Photonics* **3**, 297 (2009).
- <sup>2</sup>J. Hou, H. Y. Chen, S. Zhang, R. I. Chen, Y. Yang, Y. Wu, and G. Li, *J. Am. Chem. Soc.* **131**, 15586 (2009).
- <sup>3</sup>Y. Liang, Y. Wu, D. Q. Feng, S. T. Tsai, H. J. Son, G. Li, and L. P. Yu, *J. Am. Chem. Soc.* **131**, 7792 (2009).
- <sup>4</sup>H. Y. Chen, J. Hou, S. Zhang, Y. Liang, G. Yang, Y. Yang, L. Yu, Y. Wu, and G. Li, *Nat. Photonics* **3**, 649 (2009).
- <sup>5</sup>F. C. Chen, J. L. Wu, C. L. Lee, W. C. Huang, H. M. P. Chen, and W. C. Chen, *IEEE Electron Device Lett.* **30**, 727 (2009).
- <sup>6</sup>S. K. Hau, H. L. Yip, N. S. Baek, J. Y. Zou, K. O'Malley, and A. K. Y. Jen, *Appl. Phys. Lett.* **92**, 253301 (2008).
- <sup>7</sup>H. H. Liao, L. M. Chen, Z. Xu, G. Li, and Y. Yang, *Appl. Phys. Lett.* **92**, 173303 (2008).
- <sup>8</sup>M. S. White, D. C. Olson, S. E. Shaheen, N. Kopidakis, and D. S. Ginley, *Appl. Phys. Lett.* **89**, 143517 (2006).
- <sup>9</sup>R. Steim, S. A. Choulis, P. Schilinsky, and C. J. Brabec, *Appl. Phys. Lett.* **92**, 093303 (2008).
- <sup>10</sup>D. W. Zhao, P. Liu, X. W. Sun, S. T. Tan, L. Ke, and A. K. K. Kyaw, *Appl. Phys. Lett.* **95**, 153304 (2009).
- <sup>11</sup>F. C. Chen, J. L. Wu, C. L. Lee, Y. Hong, C. H. Kuo, and M. H. Huang, *Appl. Phys. Lett.* **95**, 013305 (2009).
- <sup>12</sup>S. I. Na, K. Seok-Soon, S. S. Kwon, J. Jang, K. Juhwan, T. Lee, and K. Dong-Yu, *Appl. Phys. Lett.* **91**, 173509 (2007).
- <sup>13</sup>C. F. Zhang, S. W. Tong, C. Y. Jiang, E. T. Kang, D. S. H. Chan, and C. X. Zhu, *Appl. Phys. Lett.* **93**, 043307 (2008).
- <sup>14</sup>J. Gilot, I. Barbu, M. M. Wienk, and R. A. J. Janssen, *Appl. Phys. Lett.* **91**, 113520 (2007).
- <sup>15</sup>J. Y. Kim, S. H. Kim, H. H. Lee, K. Lee, W. L. Ma, X. Gong, and A. J. Heeger, *Adv. Mater.* **18**, 572 (2006).
- <sup>16</sup>A. Roy, S. H. Park, S. Cowan, M. H. Tong, S. N. Cho, K. Lee, and A. J. Heeger, *Appl. Phys. Lett.* **95**, 013302 (2009).
- <sup>17</sup>T. Ameri, G. Dennler, C. Waldauf, P. Denk, K. Forberich, M. C. Scharber, C. J. Brabec, and K. Hingerl, *J. Appl. Phys.* **103**, 084506 (2008).
- <sup>18</sup>C. Tao, S. P. Ruan, X. D. Zhang, G. H. Xie, L. Shen, X. Z. Kong, W. Dong, C. X. Liu, and W. Y. Chen, *Appl. Phys. Lett.* **93**, 193307 (2008).
- <sup>19</sup>G. Li, V. Shrotriya, J. S. Huang, Y. Yao, T. Moriarty, K. Emery, and Y. Yang, *Nature Mater.* **4**, 864 (2005).
- <sup>20</sup>V. Shrotriya, G. Li, Y. Yao, T. Moriarty, K. Emery, and Y. Yang, *Adv. Funct. Mater.* **16**, 2016 (2006).
- <sup>21</sup>L. A. A. Pettersson, L. S. Roman, and O. Inganäs, *J. Appl. Phys.* **86**, 487 (1999).
- <sup>22</sup>K. Kawano, N. Ito, T. Nishimori, and J. Sakai, *Appl. Phys. Lett.* **88**, 073514 (2006).
- <sup>23</sup>B. V. Andersson, D. M. Huang, A. J. Moulé, and O. Inganäs, *Appl. Phys. Lett.* **94**, 043302 (2009).
- <sup>24</sup>F. Monestier, J. J. Simon, P. Torchio, L. Escoubas, F. Florya, S. Bailly, R. de Bettignies, S. Guillerez, and C. Defranoux, *Sol. Energy Mater. Sol. Cells* **91**, 405 (2007).
- <sup>25</sup>A. J. Moulé and K. Meerholz, *Appl. Phys. B: Lasers Opt.* **92**, 209 (2008).